

# Charge-density-wave formation by Van Hove nesting in the $\alpha$ -phase of Sn/Ge(111)

J. González

*Instituto de Estructura de la Materia. Consejo Superior de Investigaciones Científicas. Serrano 123, 28006 Madrid. Spain.*  
(November 5, 2018)

We study the role of electron correlations in the formation of the surface charge-density-wave state in the Sn/Ge(111) interface. The Fermi energy of the overlayer is treated as a dynamical variable, which undergoes a substantial renormalization by the interaction. We show that the Fermi level turns out to be pinned to a Van Hove singularity in the density of states, which explains the formation of the charge-density-wave, the observation of a very flat band in photoemission experiments and the reduction of the spectral weight in the low-temperature phase.

The formation of states with rearrangement of the electronic charge is accompanied in general by interesting properties in condensed matter systems. A recent example has been provided by the study of interfaces like Pb/Ge(111) [1,2], Sn/Ge(111) [3,4] or K/Si(111) [5]. All of them have in common the existence of a phase transition with the formation of a surface charge-density-wave (CDW) in the low-temperature phase. In the first two cases the adsorbate phases have at room temperature the same  $(\sqrt{3} \times \sqrt{3})R30^\circ$  structure, and they both show a reduction of the symmetry to a  $(3 \times 3)$  ground state below the critical temperature. However, while the Pb/Ge(111) overlayer becomes insulating in the charge-ordered state, the Sn/Ge(111) remains metallic below the transition. In the first case, the analysis of the surface band has revealed nesting along significant portions of the two-dimensional Fermi surface [1], which would account for the formation of the CDW. In the  $\alpha$ -phase of Sn/Ge(111), however, no similar effect seems to be at work [3,4], and the reason why the ground state of the system is led to reorder its charge is not fully understood yet.

It is believed that correlation effects may play an important role in the development of the charge-ordered state [6,7]. The relatively small surface bandwidth of these systems ( $\sim 0.5$  eV) leads to consider the on-site Coulomb repulsion as one of the relevant interactions. It has been also suggested that a nearest-neighbor repulsion may play an important role in producing the  $3 \times 3$  surface periodicity [6].

In this letter we develop the idea that the electron correlations are essential to understand the low-temperature phase of Sn/Ge(111), while relying on the fact that no strong-coupling effects need to be invoked for that purpose. This is plausible as long as the overlayer remains metallic below the transition. We will show that the  $(\sqrt{3} \times \sqrt{3})$  phase is unstable towards the formation of saddle points near the Fermi surface in the electronic dispersion relation. This is in agreement with the observation of a very flat band below the Fermi level in the angle-resolved photoemission experiments carried out in the CDW phase [4]. The Van Hove singularity controls

the dynamics of the system since, as we will see, this finds energetically favorable to readjust the bands in order to place the Fermi surface closer to the saddle points. As well as nesting of the saddle points near the Fermi surface gives rise to a spin-density-wave instability in the repulsive  $t - t'$  Hubbard model [8–12], it is able to explain the formation of the CDW under the assumption of a more general interaction in the present instance.

We will take an extended Hubbard model with on-site  $U$  and nearest-neighbor  $V$  repulsive interactions on the triangular lattice of the Sn/Ge(111) overlayer to illustrate these ideas. The adatom dangling bonds give rise to a band that reaches a minimum at the corner of the hexagonal  $(\sqrt{3} \times \sqrt{3})$  Brillouin zone, and a maximum close to the center [3]. We use a tight-binding approximation with nearest neighbor hopping  $t$  and next-to-nearest neighbor hopping  $t'$  to parametrize the Fermi line of the  $(\sqrt{3} \times \sqrt{3})$  phase as given in Ref. [3]. Although the precision of the fit to the dispersion relation is limited with this approximation, we are able to capture in this way the main topological features, which play an essential role in the following considerations.

The topology of the dispersion relation is actually unstable under the smallest periodic lattice distortion. This has to be taken into account, as it has been recently observed that one of the Sn atoms in the  $(3 \times 3)$  unit cell is slightly displaced upwards with respect to the other two [13,14]. By taking a hopping parameter equal to  $0.9t$  between inequivalent Sn atoms in the  $(3 \times 3)$  unit cell, we already observe the appearance of two subbands of very different character. The original valence band for the  $(\sqrt{3} \times \sqrt{3})$  lattice splits along the  $\Gamma K$  direction of the  $(3 \times 3)$  Brillouin zone. Thus, there are an upper and a lower subband that join at the apex of the conical dispersion shown in Fig. 1, characteristic of the underlying honeycomb lattice, and a middle subband that develops a saddle point at the boundary of the Brillouin zone, as shown in Fig. 2. The density of states redistributes itself, having a linear dependence in energy near K in the upper and lower honeycomb-type subbands while becoming divergent at the M point in the middle subband.

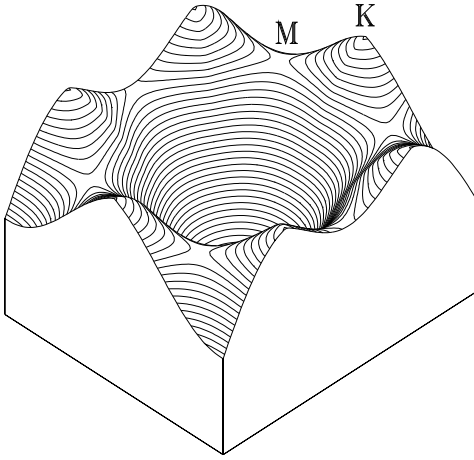


FIG. 1. Lower subband of the  $(3 \times 3)$  phase. The upper subband (not shown) displays symmetric cusps at the six corners of the  $(3 \times 3)$  Brillouin zone.

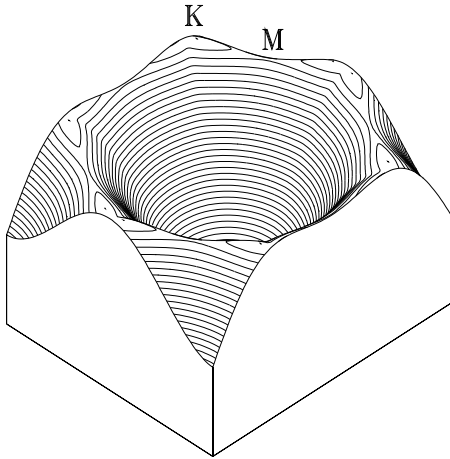


FIG. 2. Middle subband of the  $(3 \times 3)$  phase. The saddle points lie at the boundary of the  $(3 \times 3)$  Brillouin zone.

Before switching the interaction, the Fermi level has a nominal location below the mentioned Van Hove singularity. However, the relative position of the Fermi level in the different subbands of the model may suffer significant changes by the effect of the electron correlations near the singularity. The forward scattering vertex  $\Gamma_{\text{fwd}}$  giving the four-point interaction at small momentum transfer  $\mathbf{k}$  gets corrected by the iteration of the particle-hole polarizability. For the saddle-point dispersion relation  $\varepsilon(\mathbf{k}) \approx k_x^2 - k_y^2$ , this object diverges in the static limit as  $\sim \log(\Lambda/\max\{|\varepsilon(\mathbf{k})|, |\varepsilon_F|\})$ , where  $\varepsilon_F$  is the distance of the Fermi level to the Van Hove singularity and  $\Lambda$  is a cutoff of the order of the bandwidth [15]. In the case of a spin-independent interaction, this leads to a reduction of the vertex at zero momentum-transfer

$$\Gamma_{\text{fwd}}(\varepsilon_F) = \frac{U_{\text{fwd}}}{1 + (c/(2\pi^2\Lambda))U_{\text{fwd}} \log|\Lambda/\varepsilon_F|} \quad (1)$$

where the bare coupling is  $U_{\text{fwd}} \equiv U(\mathbf{p}_1, \mathbf{p}_2; \mathbf{p}_1, \mathbf{p}_2) - U(\mathbf{p}_1, \mathbf{p}_2; \mathbf{p}_2, \mathbf{p}_1)$ , in terms of the original four-fermion interaction, and  $c$  is the prefactor of the particle-hole polarizability [16]. This renormalization of  $\Gamma_{\text{fwd}}$  has important consequences, since it encodes the sum of dominant logarithmic contributions that give rise to the constant shift of the chemical potential in the self-energy corrections [17]. In this respect, it has been shown that the Van Hove singularity has a natural tendency to pin the Fermi level in a model with bare repulsive interactions [18,19]. In the present case, this can be understood in terms of the uneven screening of the forward scattering in the different subbands of the model, as we show in what follows.

Let us model the problem of the interaction between the two subbands in Figs. 1 and 2 by taking the divergent density of states near the saddle-point structure

$$n^{(1)}(\varepsilon) = -\frac{1}{\Lambda} \log(|\varepsilon|/\Lambda), \quad -\Lambda < \varepsilon < \Lambda \quad (2)$$

and a vanishing density of states for the lower subband

$$n^{(2)}(\varepsilon) = \frac{\alpha}{\Lambda^2} |\varepsilon|, \quad -\beta\Lambda < \varepsilon < \beta\Lambda \quad (3)$$

The physical value of the Fermi energy comes from the balance between the nominal value  $\mu$  of the chemical potential and the shift of the one-particle levels to higher energies due to the repulsive interaction. The filling level of each subband is determined by the self-energy corrections, bearing in mind that the upward displacement of the levels depends in turn on the charge present in all the subbands. The filling level  $\varepsilon_{F1}$  in the middle subband is given by the equation

$$\varepsilon_{F1} = \mu - \Gamma_{\text{fwd}}(\varepsilon_{F1}) \int^{\varepsilon_{F1}} d\varepsilon n^{(1)}(\varepsilon) - g_{\text{fwd}} \int^{\varepsilon_{F2}} d\varepsilon n^{(2)}(\varepsilon) \quad (4)$$

where we have introduced a coupling constant  $g_{\text{fwd}}$  that parametrizes the Coulomb repulsion exerted on the middle subband by the charge present in the lower subband. Analogously, the filling level  $\varepsilon_{F2}$  in the latter is computed in the form

$$\varepsilon_{F2} = \mu - U_{\text{fwd}} \int^{\varepsilon_{F2}} d\varepsilon n^{(2)}(\varepsilon) - g_{\text{fwd}} \int^{\varepsilon_{F1}} d\varepsilon n^{(1)}(\varepsilon) \quad (5)$$

We remark that  $\varepsilon_{F1}$  and  $\varepsilon_{F2}$  are measured in the reference frames in which the dependences  $n^{(1)}(\varepsilon)$  and  $n^{(2)}(\varepsilon)$  are as given in Eqs. (2) and (3). Thus, the fact that  $\varepsilon_{F1}$  and  $\varepsilon_{F2}$  are nominally different after renormalization is just an artifact of that convention. The physical picture is however the opposite, namely that the one-particle levels are shifted to higher energy by a different amount in each of the subbands, up to a point in which the respective Fermi levels reach the common chemical potential.

The coupled set of equations (4) and (5) gives rise to nontrivial physical effects, as a consequence of the nonlinearities introduced by the divergent density of states  $n^{(1)}(\varepsilon)$  and the renormalization of  $\Gamma_{\text{fwd}}(\varepsilon)$  close to the Van Hove singularity. It is convenient to solve for the location of  $\varepsilon_{F1}$  and  $\varepsilon_{F2}$  in terms of the total charge  $N$  in the system, given by

$$N = \int^{\varepsilon_{F1}} d\varepsilon n^{(1)}(\varepsilon) + \int^{\varepsilon_{F2}} d\varepsilon n^{(2)}(\varepsilon) \quad (6)$$

The most remarkable effect is that there is not a one-to-one correspondence between  $N$  and the respective filling levels  $\varepsilon_{F1}$  and  $\varepsilon_{F2}$  for the two subbands. The different branches of the solution are represented in Fig. 3 for the particular values  $U_{\text{fwd}} = 4.0\Lambda$  and  $g_{\text{fwd}} = 3.0\Lambda$ . The parameter  $\beta$  has been chosen equal to 3.0, and  $\alpha$  has been set so that there is the same number of states in the lower and in the middle subband.

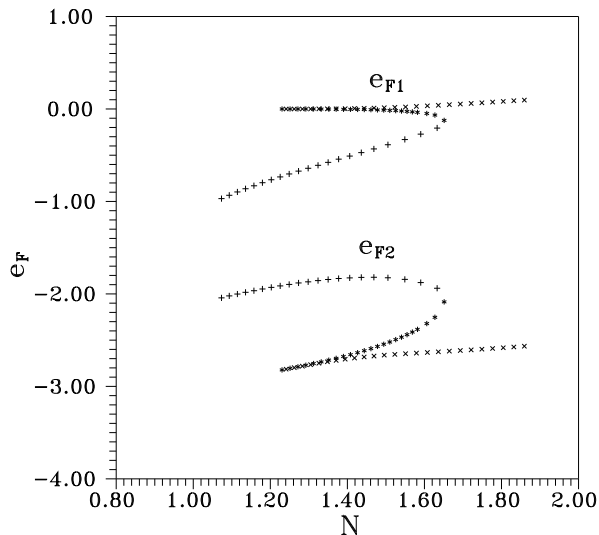


FIG. 3. Self-consistent solutions for the filling levels in the middle and lower subbands vs total charge  $N$  in the overlayer.

At low values of  $N$ , the filling of the middle subband with the Van Hove singularity proceeds in a regular way, with a monotonous increase of  $\varepsilon_{F1}$ . There is a point, however, in which two other locations of  $\varepsilon_{F1}$  become possible, closer to the singularity in the density of states. In these instances, the corresponding filling level  $\varepsilon_{F2}$  in the second subband suffers an abrupt decrease with respect to the expected value. It is interesting to discern what of the possible solutions is most favorable energetically. We have plotted in Fig. 4 the value of the total energy  $E$  versus the total charge  $N$ . We see that above a certain value, that is  $N \approx 1.4$  in our case, any of the two filling levels close to the Van Hove singularity give the most stable configuration of the system. This is in agreement with previous analyses of the pinning of the Fermi level of electrons near a Van Hove singularity [18,19].

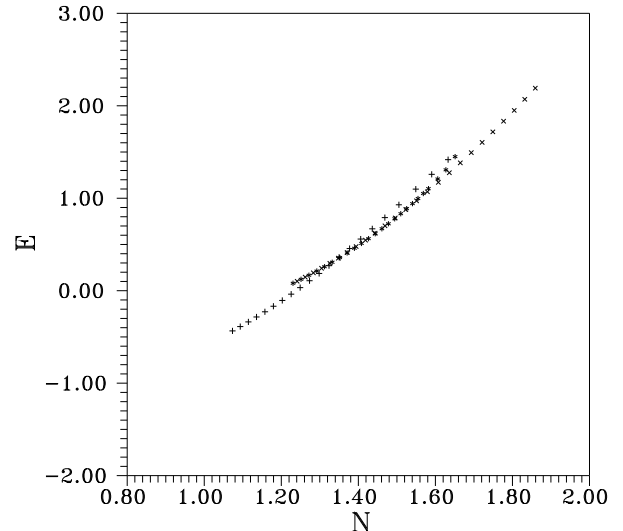


FIG. 4. Total energy of the different solutions shown in Fig. 3 vs total charge  $N$  (the symbols for a given solution match in the two figures).

The result that turns out to be valid under very general conditions is the existence of an intermediate range of filling levels that are forbidden below the Van Hove singularity. For the corresponding values of the charge  $N$ , this finds more favorable to fill the Fermi sea up to the Van Hove singularity, at the expense of the charge in the other subband. In general, there is a critical value of  $N$  in which the filling level  $\varepsilon_{F1}$  jumps discontinuously from the regular evolution upon doping to a position much closer to the Van Hove singularity.

Coming back to the physics of the Sn/Ge(111) overlayer, a description consistent with the plots in Figs. 1 and 2 leads to a nominal value of  $\varepsilon_{F1}$  that is about 25% off the Van Hove singularity, relative to the energy difference between the level of the latter and the bottom of the subband. This nominal value falls certainly in the forbidden region, what leads us to conclude according to the above arguments that the Fermi level is pinned close to the Van Hove singularity developed in the system.

This abrupt renormalization of the Fermi level towards the Van Hove singularity is able to account for all the prominent experimental features found in the Sn/Ge(111) interface, as we show in what follows.

#### 1. Strong correlations in the low-temperature phase.

The different photoemission experiments have in common the observation in the low-temperature phase of a lower band that disperses along the  $\Gamma M$  direction of the  $(3 \times 3)$  Brillouin zone, together with another band with higher energy and much less dispersion [4,13]. The point is that this intermediate band is found at an energy sensibly lower than predicted by LDA calculations [13]. Quite remarkably, all the points along the  $\Gamma M$  direction are found below the Fermi level. After taking into account the experimental overestimation of the binding energies

remarked in Ref. [4], the M point turns out to be close but *below* the Fermi level, contrary to the estimates carried out neglecting many-body effects. This is actually the experimental signature of the pinning to the Van Hove singularity we have discussed above.

It is also clear that the width of the middle subband is sensibly smaller than predicted by LDA calculations [4,13]. This reduction in the bandwidth is also consistent with the renormalization of the kinetic energy of electrons close to a saddle point, which leads to a flatter shape of the dispersion relation [15].

## 2. Formation of the surface CDW.

The saddle points of the middle subband are at the M points of the  $(3 \times 3)$  Brillouin zone, so that they are separated by momenta  $\mathbf{K}_i$  that correspond actually to the wavevectors of the CDW structure observed experimentally. This Van Hove nesting by momenta  $\mathbf{K}_i$  connecting the saddle points near the Fermi level leads to the CDW instability.

In the context of an extended Hubbard model and with the inclusion of the electron-phonon interaction, it has been shown that it is natural to have a negative coupling  $U_{\mathbf{K}_i}$  for the four-fermion interaction with momentum transfer  $\mathbf{K}_i$  [6] (its bare value is actually  $U - 6V$ , in terms of the parameters of the extended Hubbard model). We remark that, with a divergent density of states close to the Fermi level, the slightest attractive interaction ( $U_{\mathbf{K}_i} < 0$ ) triggers the CDW instability. The particle-hole susceptibility with momentum  $\mathbf{K}_i$  is itself logarithmically divergent, and the iteration of particle-hole diagrams leads to an effective vertex at momentum transfer  $\mathbf{K}_i$

$$\Gamma_{\mathbf{K}_i}(\varepsilon) = \frac{U_{\mathbf{K}_i}}{1 + (c'/(2\pi^2\Lambda))U_{\mathbf{K}_i} \log |\Lambda/\varepsilon|} \quad (7)$$

Thus, the attractive interaction is overscreened and renormalized towards more intense attraction at low energies.

Under these conditions, the only response function that shows a divergence at some critical frequency corresponds to a charge modulation with wavevectors  $\mathbf{K}_i$ . The gap that opens up at the saddle points can be actually estimated from the frequency at which the denominator in Eq. (7) vanishes. The order of magnitude thus obtained (tens of meV) is consistent with the temperature of the transition to the CDW.

## 3. Metallic behavior and depletion of the density of states in the low-temperature phase.

The metallic behavior of the  $(3 \times 3)$  phase follows naturally from our description of the different subbands in the system. Nesting of the saddle points at the Van Hove filling and the formation of the surface CDW lead to the opening of a gap and to a partial destruction of the Fermi line around the saddle points [20]. The divergent density

of states induces by itself a significant reduction of the quasiparticle weight, as appreciated in the computation of the self-energy corrections for the saddle point dispersion relation [15]. This is consistent with the decrease of the photoemission intensity about the Fermi level observed in the CDW phase [4]. The lower band is less sensitive to these renormalization effects, and the metallic properties come mainly from the band crossing the Fermi level below the cusps shown in Fig. 1.

In conclusion, the pinning of the Fermi level to a Van Hove singularity in the density of states leads to a phenomenology for the Sn/Ge(111) overlayer consistent with the experimental observations of CDW formation and photoemission measurements, which are challenging more conventional theoretical approaches. Further predictions of our approach should also be tested experimentally in Sn/Ge(111), in particular the renormalization of the lower band and the geometry of the Fermi line around the corners of the  $(3 \times 3)$  Brillouin zone.

- 
- [1] J. M. Carpinelli, H. H. Weitering, E. W. Plummer and R. Stumpf, *Nature* **381**, 398 (1996).
  - [2] A. Goldoni, C. Cepek and S. Modesti, *Phys. Rev. B* **55**, 4109 (1997).
  - [3] J. M. Carpinelli *et al.*, *Phys. Rev. Lett* **79**, 2859 (1997).
  - [4] A. Goldoni and S. Modesti, *Phys. Rev. Lett* **79**, 3266 (1997).
  - [5] H. H. Weitering *et al.*, *Phys. Rev. Lett.* **78**, 1331 (1997).
  - [6] G. Santoro *et al.*, *Surf. Sci.* **404**, 802 (1998).
  - [7] S. Scandolo *et al.*, *Surf. Sci.* **404**, 808 (1998).
  - [8] R. S. Markiewicz, *J. Phys. Chem. Sol.* **58**, 1179 (1997).
  - [9] L. B. Ioffe and A. J. Millis, *Phys. Rev. B* **54**, 3645 (1996).
  - [10] J. V. Alvarez *et al.*, *J. Phys. Soc. Jpn.* **67**, 1868 (1998).
  - [11] M. Murakami and H. Fukuyama, *J. Phys. Soc. Jpn.* **67**, 2784 (1998).
  - [12] C. J. Halboth and W. Metzner, *Phys. Rev. B* **61**, 7364 (2000).
  - [13] J. Avila *et al.*, *Phys. Rev. Lett.* **82**, 442 (1999).
  - [14] O. Bunk *et al.*, report cond-mat/9909283.
  - [15] J. González, F. Guinea and M. A. H. Vozmediano, *Nucl. Phys.* **B485**, 694 (1997).
  - [16] J. González, F. Guinea and M. A. H. Vozmediano, report cond-mat/9905166, to be published in *Phys. Rev. Lett.*
  - [17] Momentum dependence is carried however by the subdominant terms, which are responsible of a mild correction of the shape of the saddle-point dispersion relation.
  - [18] R. S. Markiewicz, *J. Phys.: Condens. Matter* **2**, 665 (1990).
  - [19] J. González, F. Guinea and M. A. H. Vozmediano, *Europhys. Lett.* **34**, 711 (1996).
  - [20] N. Furukawa, T. M. Rice and M. Salmhofer, *Phys. Rev. Lett.* **81**, 3195 (1998).